Numerical Approach of Coupling Vibration Magneto-convection In Nanofluid

S Kadri[1]*, M Elmir[2], R Mehdaoui[2]

1. LPDS Laboratory, Exact Sciences Faculty, TAHRI Mohamed University, Bechar, Algeria

2. ENERGARID Laboratory, Technology Faculty, TAHRI Mohamed University, Bechar, Algeria

ABSTRACT

The objective of our work is to visualize numerically the effect of coupling vibratory excitation and magnetic field on cooling an electronic component or a solar cell (originality of our study) in arid and semi-arid area. A square cavity of side H filled with Al_2O_3-water nanofluid where an electronic component is placed on the bottom horizontal wall is maintained at isothermal hot temperature Th. The top horizontal wall is maintained at a cold temperature Tc. The vertical walls are adiabatic. The equations describing the natural convection flow in the square cavity consist of mass conservation, momentum and energy. For the physical parameters of Al_2O_3-water nanofluid, we use the Brinkman and Wasp model. Transport equations are solved numerically by finite element method. The results are obtained for Rayleigh number Ra= 105, Hartmann numbers between 0 and 100 and vibratory excitation inclination angle between 0° and 90°. The external magnetic field inclination angle varies between 0° and 90° and the Rayleigh number ratio between 0 and 50. Results are presented in the form of heat transfer flux ratio and maximum absolute value of stream function.

1. INTRODUCTION

The coupling vibration magneto-convection in nanofluid has importance in several areas such as the cooling of electronic systems, power generation, air conditioning, microelectronics. The topic of natural convection in a cavity is of importance because many engineering applications, heating and/or cooling takes place inside the enclosure [1]. In the literature, a rich and variety of numerical results have been published on the phenomenon of natural convection in differentially heated shallow enclosures with various wall conditions [2-10].

The study of magnetic field effects has attracted attentions of engineers and science due to its wide industrial applications. The problem of heat transfer in the presence of a magnetic field attracts the attention of researchers for a long time. It is little work for nanofluids compared to fluids and liquid metals. Ece and Buyuk [11] illustrated the natural convection flow under a magnetic field in an inclined rectangular cavity for heated and cooled on the adjacent walls. Mahmud and Fraser [12] have investigated magneto-hydrodynamic natural convection flow and entropy generation in a square cavity. On the contrary Grosan et al. [13] has studied effects of magnetic field and internal heat generation on natural convection flow in rectangular cavity filled with porous medium. Pirmohammadi et al. [14] studied the effect

*Corresponding Author: syhammiss@yahoo.fr

of a magnetic field on buoyancy-driven convection in differentially heated square enclosure. They showed that the heat transfer mechanisms and the flow characteristics inside the enclosure depend strongly upon both the strength of the magnetic field as well as the Rayleigh number. Recently, H.R. Ashorynejad et al. [15] were investigated numerically the effect of static radial magnetic field on natural convection heat transfer in a horizontal cylindrical annulus enclosure filled with nanofluid using the Lattice Boltzmann method (LBM). They found that the overage Nusselt number is an increasing function of nanoparticles volume fraction and Rayleigh number, while it is a decreasing function of Hartmann number. Mahmoudi et al. [16] studied the MHD natural convection and entropy generation in a trapezoidal enclosure using Cu–water nanofluid. They found that at Ra =10^4 and 10^5 the enhancement of the Nusselt number due to presence of nanoparticles increases with the Hartman number, but at higher Rayleigh number, a reduction has been observed. In addition, it was observed that the entropy generation is decreased when the nanoparticles are present, while the magnetic field generally increases the magnitude of the entropy generation.

Vibrations are known to be among the most effective ways of affecting the behavior of fluid systems in the sense of increasing or reducing the convective heat transfer. The study of vibrations to the fluid has been the subject of several works, which is not the case for nanofluids [17-22].

The objective of our work is to increase the rate of transfer by coupling vibration magneto-convection to facilitate proper cooling of the electronic component or solar cell and increase their efficiency.

2. MATHEMATICAL MODEL

The configuration studied is shown in Figure 1. It is mainly based on a square cavity of side H filled with Al_2O_3-water nanofluid in natural convection. This medium is heated from below and subjected to inclined vibratory excitation and an inclined external magnetic field. The vertical walls are adiabatic and impermeable. The horizontal walls are maintained at constant temperatures and uniform Tc and Th at y = 0 and y = H respectively. In the present analysis, Cartesian coordinate system will be applied. The temperatures of the vertical walls have been considered to be insulated. An electronic compounds or a solar cell is placed in the bottom horizontal wall. The nanofluid is Newtonian, incompressible, and the flow is laminar. The induced magnetic field is assumed to be negligible with respect to the applied magnetic field parallel to gravity. Moreover, it is assumed that both fluid phase and nanoparticles are in thermal equilibrium state and they flow at the same velocity. The Boussinesq approximation is assumed to be valid.

The nondimensional version of the governing system of transport equations are as follow:

$$\frac{\partial u}{\partial x}+\frac{\partial v}{\partial y}=0 \tag{1}$$

$$\frac{\partial u}{\partial t}+u\frac{\partial u}{\partial x}+v\frac{\partial u}{\partial y}=-\frac{1}{\rho_{nf}}\frac{\partial P}{\partial x}+\frac{\mu_{eff}}{\rho_{nf}}\left(\frac{\partial^2 u}{\partial x^2}+\frac{\partial^2 u}{\partial y^2}\right)-(1-\beta_{nf}\Delta T)bw^2\cos\Phi$$
$$-\frac{\sigma_{nf}B^2}{\rho_{nf}}\left(v\sin\theta\cos\theta-u\sin^2\theta\right) \tag{2}$$

$$\frac{\partial v}{\partial t}+u\frac{\partial v}{\partial x}+v\frac{\partial v}{\partial y}=-\frac{1}{\rho_{nf}}\frac{\partial P}{\partial y}+\frac{\mu_{eff}}{\rho_{nf}}\left(\frac{\partial^2 v}{\partial x^2}+\frac{\partial^2 v}{\partial y^2}\right)-(1-\beta_{nf}\Delta T)\left(g-bw^2\sin\Phi\sin(wt)\right)$$
$$-\frac{\sigma_{nf}B^2}{\rho_{nf}}\left(u\sin\theta\cos\theta-v\cos^2\theta\right) \tag{3}$$

$$\frac{\partial T}{\partial t}+u\frac{\partial T}{\partial x}+v\frac{\partial T}{\partial y}=\alpha_{nf}\left(\frac{\partial^2 T}{\partial x^2}+\frac{\partial^2 T}{\partial y^2}\right) \tag{4}$$

$$\frac{\partial^2\psi}{\partial x^2}+\frac{\partial^2\psi}{\partial y^2}=\frac{\partial u}{\partial y}-\frac{\partial v}{\partial x} \tag{5}$$

The thermal diffusivity of nanofluid is given by:

$$\alpha_{nf}=\frac{K_{nf}}{(\rho C_p)_{nf}} \tag{6}$$

The effective thermal conductivity of nanofluids is calculated using the Wasp model [23].

$$K_{nf}=K_f\frac{(2-2\varphi)K_f+(1+\varphi)K_s}{(2+\varphi)K_f+(1-\varphi)K_s} \tag{7}$$

The effective density of a fluid containing suspended particles is given by:

$$\rho_{nf}=(1-\varphi)\rho_f+\varphi\rho_s \tag{8}$$

The effective viscosity of a fluid containing a dilute suspension of small rigid spherical particles is given by Brinkman model [24] as:

$$\mu_{eff}=\frac{\mu_f}{(1-\varphi)^{2.5}} \tag{9}$$

The heat capacitance of the nanofluid can be calculated as:

$$(\rho C_p)_{nf}=(1-\varphi)(\rho C_p)_f+\varphi(\rho C_p)_s \tag{10}$$

Based upon the previous assumptions and introducing the following dimensionless variables,

$$(x^*,y^*)=\frac{(x,y)}{H},(u^*,v^*)=\frac{H(u,v)}{\alpha_f},T^*=\frac{(T-T_c)}{(T_h-T_c)},P^*=\frac{PH^2}{\rho_f\alpha_f^2},t^*=\frac{\alpha_f}{H^2}t,w^*=\frac{H^2}{\alpha_f}w$$

The governing equations for the problem in dimensionless form are as follows:

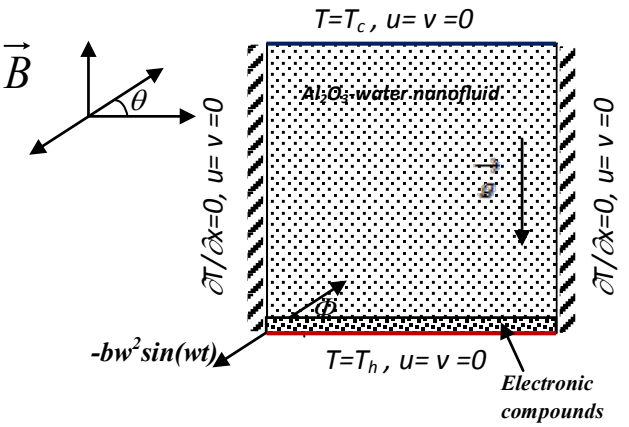

Figure 1: Physical model.

$$\frac{\partial u^*}{\partial x^*} + \frac{\partial v^*}{\partial y^*} = 0 \tag{11}$$

$$\left(1-\varphi+\varphi R_\rho\right)\left(\frac{\partial u^*}{\partial t^*} + u^*\frac{\partial u^*}{\partial x^*} + v^*\frac{\partial u^*}{\partial y^*}\right) = -\frac{\partial P^*}{\partial x^*} + \frac{\Pr}{\left(1-\varphi\right)^{2.5}}\left(\frac{\partial^2 u^*}{\partial x^{*2}} + \frac{\partial^2 u^*}{\partial y^{*2}}\right) - \left(1-\varphi+\varphi R_\rho R_\beta\right) Ra \Pr R\cos\Phi\sin\left(w^* t^*\right) T^* + \frac{\Pr Ha^{*2}}{\left(1-\varphi\right)^{2.5}}\left(v^*\sin\theta\cos\theta - u^*\sin^2\theta\right) \tag{12}$$

$$\left(1-\varphi+\varphi R_\rho\right)\left(\frac{\partial v^*}{\partial t^*} + u^*\frac{\partial v^*}{\partial x^*} + v^*\frac{\partial v^*}{\partial y^*}\right) = -\frac{\partial P^*}{\partial y^*} + \frac{\Pr}{\left(1-\varphi\right)^{2.5}}\left(\frac{\partial^2 v^*}{\partial x^{*2}} + \frac{\partial^2 v^*}{\partial y^{*2}}\right) + \left(1-\varphi+\varphi R_\rho R_\beta\right) Ra \Pr\left(1 - R\sin\Phi\sin(w^* t^*)\right) T^* + \frac{\Pr Ha^{*2}}{\left(1-\varphi\right)^{2.5}}\left(u^*\sin\theta\cos\theta - v^*\cos^2\theta\right) \tag{13}$$

$$\frac{\partial T^*}{\partial t^*} + u^*\frac{\partial T^*}{\partial x^*} + v^*\frac{\partial T^*}{\partial y^*} = \left[\frac{2+\left(\frac{1+\varphi}{1-\varphi}\right)R_k}{R_k+\left(\frac{2+\varphi}{1-\varphi}\right)}\right]\left(\frac{1}{\left(1-\varphi\right)+\varphi R_\rho}\right)\left(\frac{\partial^2 T^*}{\partial x^{*2}} + \frac{\partial^2 T^*}{\partial y^{*2}}\right) \tag{14}$$

The expressions for dimensionless parameters are given as:

$$\mathrm{Pr} = \frac{\mu_{eff}}{\rho_f \alpha_f^2},\quad Ra = \frac{\rho_f \beta_f H^3 g \Delta T}{\mu_f \alpha_f},\quad R_\rho = \frac{\rho_s}{\rho_f},\quad R_\beta = \frac{\beta_s}{\beta_f},\quad R = \frac{Rav}{Ra},\quad \mathrm{R_k} = \frac{K_s}{K_f},\quad Ha = HB\sqrt{\frac{\sigma_{nf}}{\mu_{nf}}}$$

The heat transfer is characterized by the flux ratio between nanofluid and fluid. The average flux ratio at the bottom wall is computed as follows:

$$\frac{Q_{nf}}{Q_f} = -\int_0^1 \frac{K_{nf}}{K_f}\frac{\partial T^*}{\partial y^*} \tag{15}$$

By replacing Eqn (7) in Eqn (15), we obtain:

$$\frac{Q_{nf}}{Q_f} = -\int_0^1 \left[\frac{\left(2+\left(\frac{1+\varphi}{1-\varphi}\right)R_k\right)}{R_k+\left(\frac{2+\varphi}{1-\varphi}\right)}\right]\frac{\partial T^*}{\partial y^*} \tag{16}$$

Dimensionless boundary conditions for Eqns (11)-(14) are as follows:

$u^* = v^* = 0$ and $T^* = 1$ at $y^* = 0,\quad 0 \le x^* \le 1$

$u^* = v^* = 0$ and $T^* = 0$ at $y^* = 1,\quad 0 \le x^* \le 1$

$u^* = v^* = 0$ and $\partial T^*/\partial x^* = 0$ at $x^* = 0,\quad 0 \le y^* \le 1$

$u^* = v^* = 0$ and $\partial T^*/\partial x^* = 0$ at $x^* = 1,\quad 0 \le y^* \le 1$

3. NUMERICAL METHOD AND VALIDATION

The numerical results are obtained by solving the system of steady differential Eqns (11)-(14) with appropriate boundary and initial conditions using the Galerkin finite element method. The two dimensional spatial domain is divided into quadrangle elements and a Lagrange quadratic interpolation has been chosen. Accuracy tests were performed for the steady state results using five sets of uniform grids as shown in Table 1.

Table 1: Dimensionless Boundary Conditions

Grid Sizes	Qnf/Qf	|ψ|max
21×21	2.972	5.7819
31×31	2.967	5.7837
41×41	2.964	5.784
51×51	2.964	5.784
61×61	2.964	5.784

The mesh is refined near the boundaries and we have adopted 1681 elements. The computational domain consists of bi-quadratic elements which correspond to 41×41 grid.

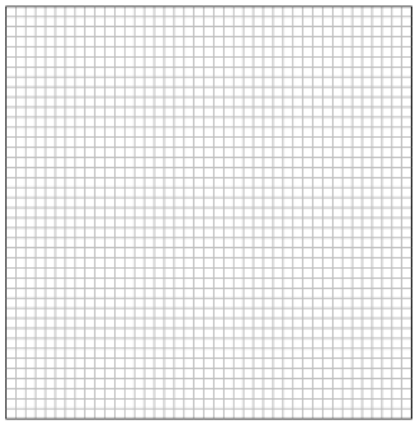

Figure 2: Optimal mesh adopted

Table 2. Validation of the numerical code in the case of Natural convection

	$Ra=10^3$	$Ra=10^4$	$Ra=10^5$	$Ra=10^6$
Present work	1.118	2.245	4.524	8.855
G.A. Sheikhzadeh et al. [8]	1.148	2.311	4.651	9.010
Khanafer et al. [25]	1.118	2.245	4.522	8.826
De Vahl Davis [26]	1.118	2.243	4.519	8.799

In order to validate our work, we will compare the results obtained with other numerical results available in the literature. The test case considered is the Natural convection flow and heat transfer in a differentially-heated square cavity filled with air. The left and the right side walls of the cavity are maintained at constant temperatures Th and Tc, respectively, with Th > Tc, while its top and bottom walls are insulated. Table 2 shows the comparison of the Nusselt number for different values of the Rayleigh number of other investigators for the same problem. As it can be observed from this table, very good agreements exist between the Nusselt numbers obtained by the present simulation and the results of Khanafer et al [25], G.A.Sheikhzadeh et al [8] and De Vahl Davis [26].

4. RESULTS AND DISCUSSION

The numerical results are presented and discussed in two half period. It sets the following parameters: φ=0.1, Ra=105, w*=25, Pr = 7, Rρ = 3.98, Rβ = 0.08 and Rk = 61.95.

First, we study the effect of the Hartmann number on the average flux ratio and the maximum absolute value of stream function for different values of the inclination angle of vibratory excitation. For this, the Hartmann number varies from 0 to 100, the magnetic field is assumed to be horizontal (θ=0°C) and the Rayleigh number ratio R=10.

The figures (3-a) and (3-b) represent the variation of the average flux ratio as a function of

the Hartmann number for different values of the inclination angle of the vibratory excitation for the first half period and the second half-period, respectively. For both curves, the average flux ratio decreases with increasing Hartmann number which leads to a decrease in heat transfer by convection. Also the increase of the inclination angle of the vibratory excitation promotes the conductive regime. Beyond the angle $\Phi = 75°$, the average flux ratio is constant which means obtaining pure conduction. By comparing the two figures, there is a discrepancy in the values of the average flux ratio indicating that the convective mode is favored in the second half period relative to the first.

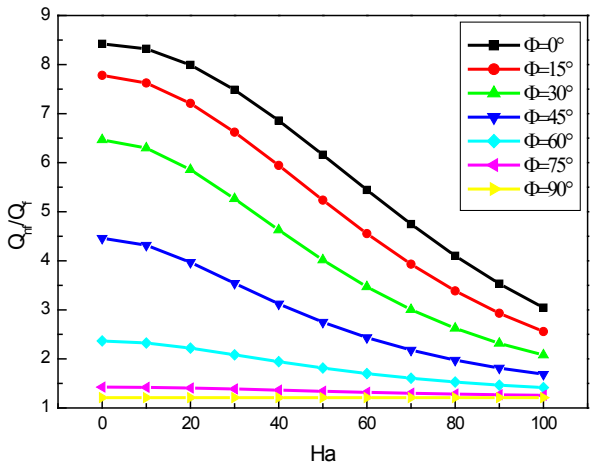

(a)

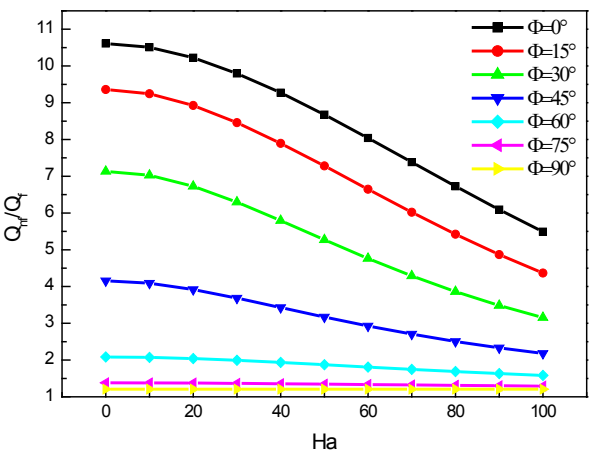

(b)

Figure 3: Variation of the average flux ratio as a function of the Hartmann number for different values of the inclination angle of the vibratory excitation for: (a) First half period and (b) second half period

Figures (4-a) and (4-b) illustrate the variation of the maximum absolute value of the stream function depending on different values of the Hartmann number for different values of the inclination angle of the vibratory excitation in the first half period and the second half period, respectively. The two curves confirm the previous results.

Second, we study the effect of the Hartmann number on the average flux ratio and the maximum absolute value of stream function for different values of the inclination angle of magnetic field. For this, the Hartmann number varies from 0 to 100, the vibratory excitation is assumed horizontal (Φ=0°C) and the Rayleigh number ratio R=10.

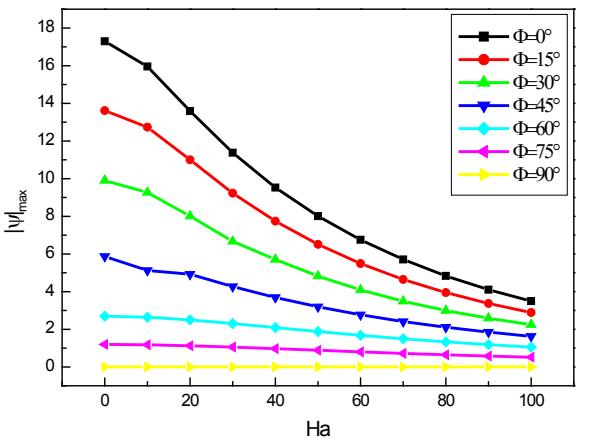

(a)

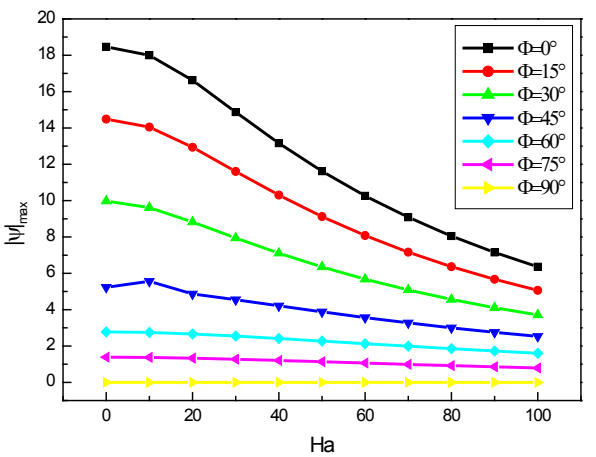

(b)

Figure 4: Variation of the maximum absolute value of the stream function depending on the Hartmann number for different values of the inclination angle of the vibratory excitation for: (a) First half period and (b) Second half period.

Figures (5-a) and (5-b) show the variation of the average flux ratio as a function of the Hartmann number for different values of the inclination angle of the magnetic field. For both curves, the average flux ratio decreases with increasing Hartmann number for all inclination angles of the magnetic field. Also the increase of the inclination angle of the magnetic field decreases heat transfer by convection. Beyond Φ=60°, the effect is almost negligible. We note that the heat exchange increases with the Hartmann number to Ha = 50. Beyond this value, the exchange is almost constant. Table 3 summarizes some results of the heat exchange rate. We conclude that the heat exchange rate is low.

Table 3. Some results of the heat exchange rate in the first half period

	Ha=30	**Ha=50**	**Ha=70**	**Ha=100**
0°- 15°	1.62%	4%	6.2%	6.3%
30°-45°	3.56%	6%	6.1%	6.2%
75°-90°	0.02%	0.95%	2%	2.5%

Figures (6-a) and (6-b) represent the evolution of the maximum absolute value of the stream function depending on the Hartmann number for different values of the inclination angle of the magnetic field for the first half period and the second half period, respectively. The two curves confirm the previous results.

In this part we study the effect of the Rayleigh number ratio R on the average flux ratio and the maximum absolute value of the stream function. For this, the ratio R varies from 0 to 50, Hartmann number Ha = 30 and the vibratory excitation is assumed horizontal (Φ=0°C).

Figures (7-a) and (7-b) show the average flux ratio as a function of the Hartmann number for different values of the inclination angle of the magnetic field for the first half period and the second half-period, respectively. We note the increase of the ratio R increases the flow ratio in both periods which promotes convective transfer mode. By increasing the ratio R, the average flux ratio increases which confirms the convective mode. As is as one increases the inclination angle of the magnetic field, the average flux ratio decreases. Beyond the temperature θ = 60° C, the inclination angle of the magnetic field has no effect on the flow and therefore report on the convective heat transfer coefficient.

Figures (8-a) and (8-b) represent the evolution of the maximum absolute value of the power function depending on the ratio of the Rayleigh numbers to different values of the angle of inclination of the magnetic field for the first half period and the second half period, respectively. The two curves confirm the previous results.

Figures (9-a) and (9-b) show the variation of the average flux ratio as a function of the ratio of the numbers of Rayleigh to different values of the inclination angle of the vibratory excitation. For both curves, and below of Φ = 45°, the average flux ratio rises with the increase of the ratio R which shows dominance convective regime. Beyond the angle Φ = 45 °, the average flux ratio decreases to a value of R = 10 which means a decrease in heat transfer by convection then becomes constant, confirming the domination of conductive mode. We can conclude a critical inclination angle near Φ=45°. For the angle Φ= 90°, we get the purely conductive regime. Also the second half period promotes convection better than the first half period.

Figures (10-a) and (10-b) illustrate the evolution of the maximum absolute value of the stream function depending on the Rayleigh numbers ratio to different values of the inclination angle of the vibratory excitation for the first half period and the second half-period, respectively. The two curves confirm the previous results.

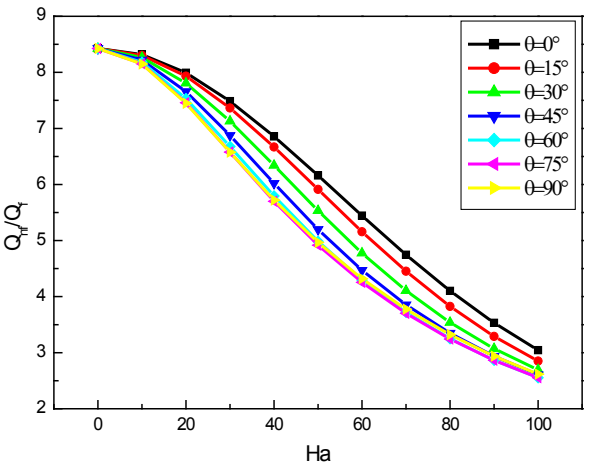

(a)

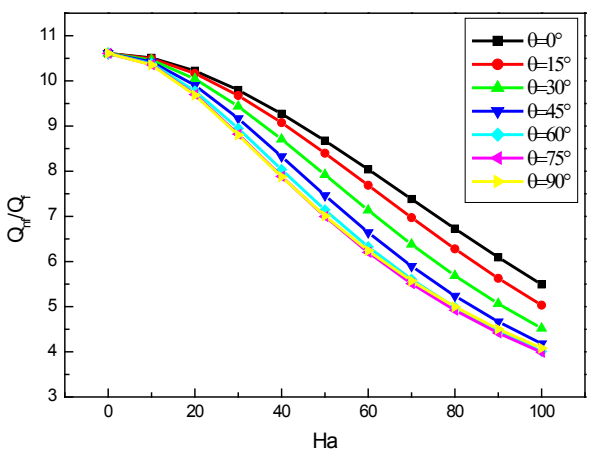

(b)

Figure 5: Variation of the average flux ratio as a function of the Hartmann number for different values of the inclination angle of the magnetic field for: (a) First half period and (b) second half period.

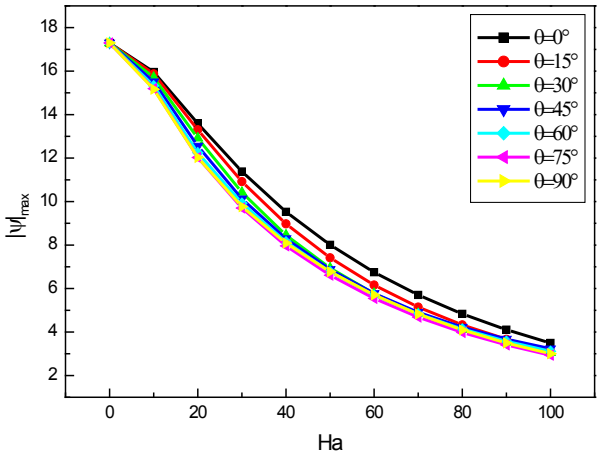

(a)

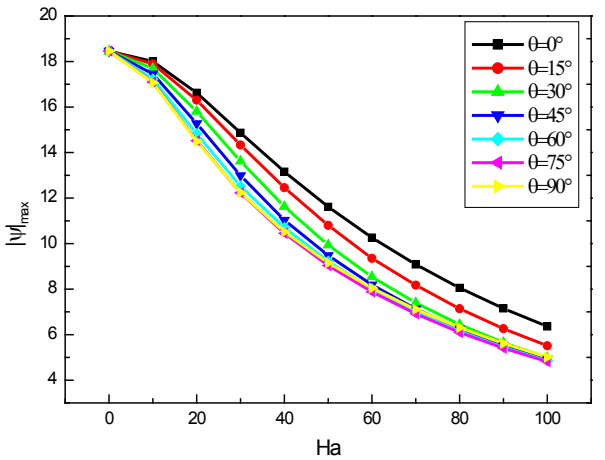

(b)

Figure 6: Variation of the maximum absolute value of the stream function depending on the Hartmann number for different values of the inclination angle of the magnetic field to (a) First half period and (b) Second half period

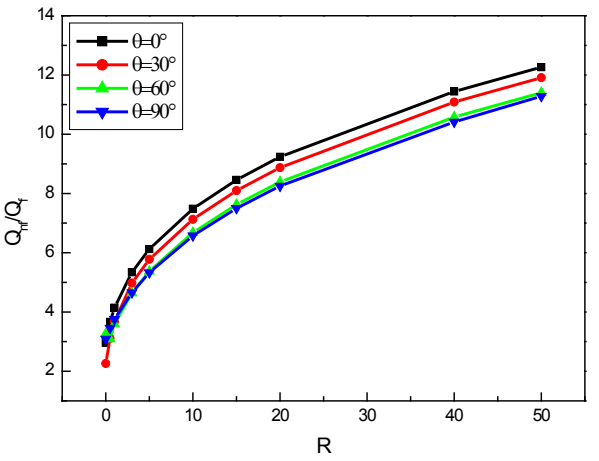

(a)

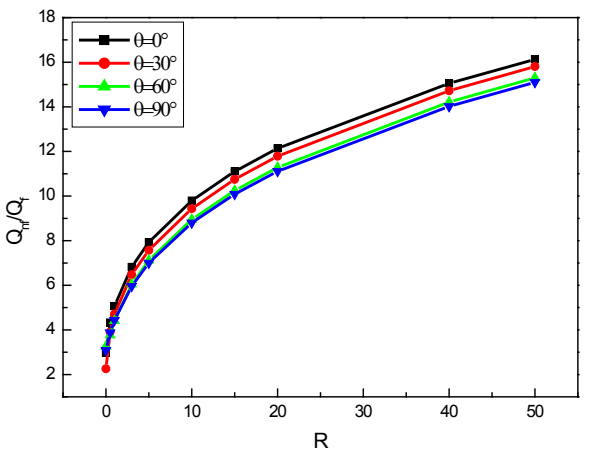

(b)

Figure 7: Variation of the average flux ratio as a function of the Hartmann number for different values of the inclination angle of the magnetic field for: (a) First half period and (b) second half period.

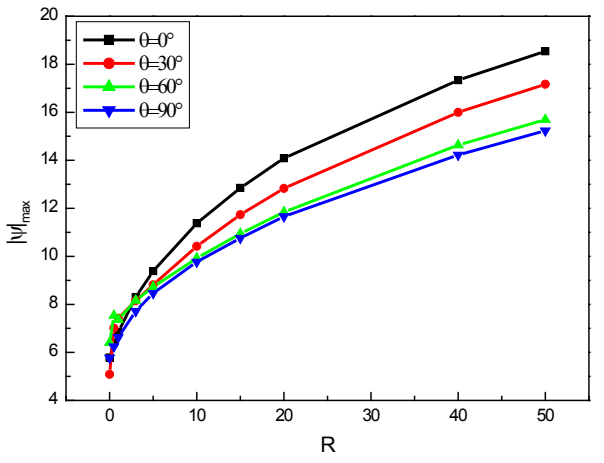

(a)

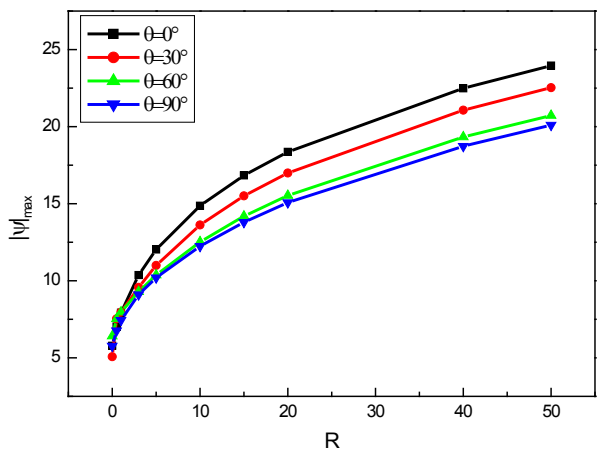

(b)

Figure 8: Variation of the maximum absolute value of the stream function depending on the Hartmann number for different values of the inclination angle of the magnetic field to (a) First half period and (b) Second half period

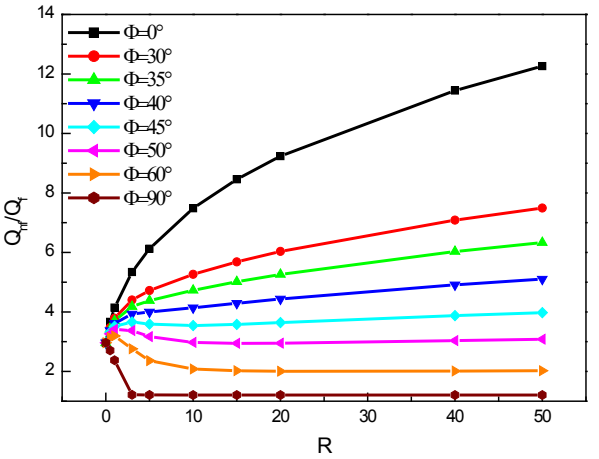

(a)

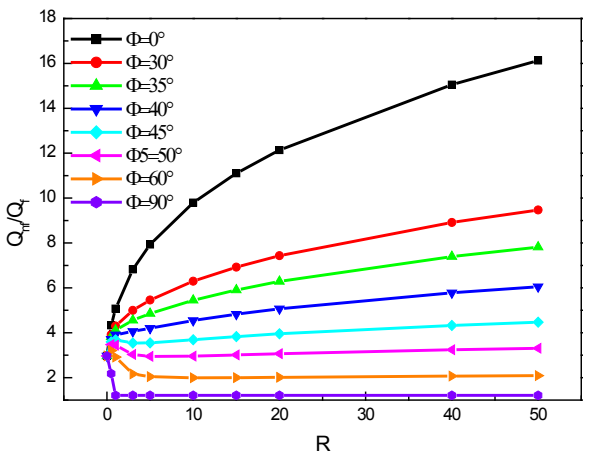

(b)

Figure 9: Variation of the average flux ratio as a function of the Hartmann number for different values of the inclination angle of the magnetic field for: (a) First half period and (b) second half period.

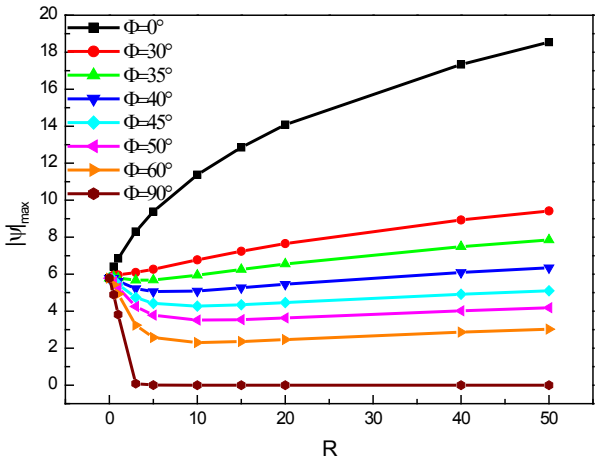

(a)

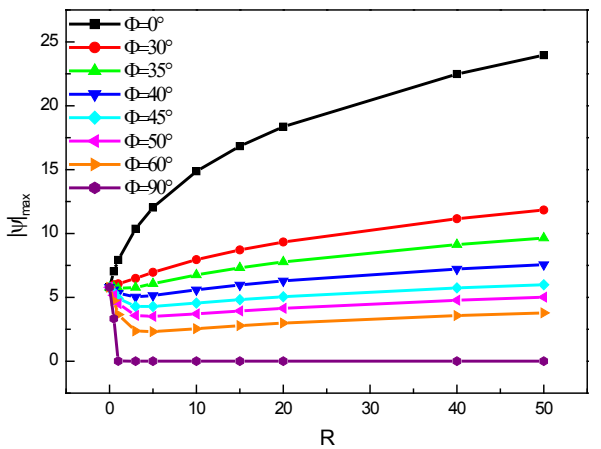

(b)

Figure 10: Variation of the maximum absolute value of the stream function depending on the Hartmann number for different values of the inclination angle of the magnetic field to (a) First half period and (b) Second half period

5. CONCLUSION

This work is devoted to study numerically the effect of coupling vibratory excitation and magnetic field on cooling an electronic component or a solar cell in cavity filled an Al_2O_3-water nanofluid. The results can deduce the following conclusions:

1- The increase Hartmann reduces the average flux ratio and the absolute value of the maximum stream function.
2- Increasing the inclination angle of the vibratory excitation promotes conductive transfer mode.
3- The effect of the inclination angle of the magnetic field minimizes the transfer of heat by convection.
4- The increase of the Rayleigh number ratio increases the average flux ratio and the absolute value of the stream function.
5- The effect of the inclination angle of the magnetic field is significant for angles $\Phi \leq 60°$.
6- In below a value of the inclination angle of the vibratory excitation of $\Phi = 45$ °, the convective regime is dominant. For against beyond this value, the conductive regime is favored.
7- The phenomenon studied presents a critical angle about 45°.

Finally for a good cooling of electronic components, it is necessary to consider the following points:

- Low numbers Hartmann
- Large values of the ratio of Rayleigh numbers
- Angles of inclination of the magnetic field lower than or equal to 60°
- Angles of inclination of vibratory excitation lower than or equal to 45°

REFERENCES

[1] Faroogh Garoosi et al., Numerical simulation of natural convection of nanofluids in a square cavity with several pairs of heaters and coolers (HACs) inside, International Journal of Heat and Mass Transfer, 2013. 67: p. 362–376.

[2] Rehena Nasrin, M.A. Alim, Free convective flow of nanofluid having two nanoparticles inside a complicated cavity, International Journal of Heat and Mass Transfer, 2013. 63: p. 191–198.

[3] Abu-Nada, H. F. Oztop, Effects of inclination angle on natural convection in enclosures filled with Cu–water nanofluid, International Journal of Heat and Fluid Flow, 2009. 30: p. 669–678.

[4] Eiyad Abu-Nada, Effects of Variable Viscosity and Thermal Conductivity of CuO-Water Nanofluid on Heat Transfer Enhancement in Natural Convection: Mathematical Model and Simulation, Journal of Heat Transfer, 2010. 132 : 1-9.

[5] S.M. Aminossadati, B. Ghasemi, Natural convection of water–CuO nanofluid in a cavity with two pairs of heat source–sink, International Communications in Heat and Mass Transfer, 2011. 38: p. 672–678.

[6] G.H.R. Kefayati et al., Lattice Boltzmann simulation of natural convection in an open enclosure subjugated to water/copper nanofluid, International Journal of Thermal Sciences, 2012. 52: p. 91-101.

[7] Z. Alloui et al., Natural convection of nanofluids in a shallow rectangular enclosure heated from the side, Can. J. Chem. Eng, 2012. 90: p. 69–78.

[8] G.A. Sheikhzadeh et al., Natural convection of Cu–water nanofluid in a cavity with partially active side walls, European Journal of Mechanics B/Fluids, 2011. 30 : p. 166–176.

[9] A.H.Mahmoudi et al., Numerical modeling of natural convection in an open cavity with two vertical thin heat sources subjected to a nanofluid, International Communications in Heat and Mass Transfer, 2011. 38: p. 110–118.

[10] E. Fattahi et al., Lattice Boltzmann simulation of natural convection heat transfer in nanofluids, International Journal of Thermal Sciences, 2012. 52: p. 137-144.

[11] M.C. Ece, E. Buyuk, Natural convection flow under magnetic field in an inclined rectangular enclosure heated and cooled on adjacent walls. Fluid Dynamics Research, 2006. 38: p. 564-590.

[12] S. Mahmud, R.A. Fraser, Magnetohydrodynamic free convection and entropy generation in a square cavity. International Journal of Heat and Mass Transfer, 2004. 47: p. 3245-3256.

[13] T. Grosan, C. Revnic, I. Pop, D.B. Ingham, Magnetic field and internal heat generation effects on the free natural convection in a rectangular cavity filled with porous medium. International Journal of Heat and Mass Transfer, 2009. 52: p. 525-1533.

[14] M. Pirmohammadi, M. Ghassemi, Effect of magnetic field on convection heat transfer inside a tilted square enclosure, International Communications in Heat and Mass Transfer, 2009. 36 : p. 776–780.

[15] Hamid Reza Ashorynejad et al., Magnetic field effects on natural convection flow of a nanofluid in a horizontal cylindrical annulus using Lattice Boltzmann method, International Journal of Thermal Sciences, 2013. 64: p. 240-250.

[16] Amir Houshang Mahmoudi et al., MHD natural convection and entropy generation in a trapezoidal enclosure using Cu–water nanofluid, Computers & Fluids, 2013. 72: p. 46–62.

[17] L. Cheng et al, Heat transfer enhancement by flow-induced vibration in heat exchangers, International Journal of Heat and Mass Transfer, 2009. 52: p. 1053–1057.

[18] A.V. Belyaev, B.L. Smorodin, The stability of ferrofluid flow in a vertical layer subject to lateral heating and horizontal magnetic field, Journal of Magnetism and Magnetic Materials, 2010. 322: p. 2596–2606.

[19] M. K. Aktas, T. Ozgumus, The effects of acoustic streaming on thermal convection in an enclosure with differentially heated horizontal walls, International Journal of Heat and Mass Transfer, 2010. 53: p. 5289–5297.

[20] F. Penot et al, Preliminary experiments on the control of natural convection in differentially-heated cavities, International Journal of Thermal Sciences, 2010. 49: p. 1911-1919.

[21] V. Shevtsova et al, Study of thermoconvective flows induced by vibrations in reduced gravity, Acta Astronautica, 2010. 66 : p. 166-173.

[22] M. Majid, P. Walze, Convection and segregation in vertically vibrated granular beds, Powder Technology, 2009. 192 : p. 311–317.

[23] Wasp, E. J., Kenny, J. P., and Gandhi, R. L., Solid-liquid Flow Slurry Pipeline Transportation, Gulf Publishing Company, Houston, Texas, 1979.

[24] Brinkman, H.C, The viscosity of concentrated suspensions and solutions J.Chem. Phys, 1952. 20: p. 571–581.

[25] K. Khanafer, K. Vafai, M. Lightstone, Buoyancy-driven heat transfer enhancement in a two-dimensional enclosure utilizing nanofluids, Int. J. Heat Mass Transfer, 2003. 46: p. 3639–3653.

[26] G. De Vahl Davis, Natural convection of air in a square cavity, a benchmark numerical solution, Internat. J. Numer. Methods Fluids, 1983. 3: p. 249–264.